

THE NATURE OF RED DWARF GALAXIES

YU WANG^{1,2}, XIAOHU YANG^{1,2}, H.J. MO³, FRANK C. VAN DEN BOSCH⁴, NEAL KATZ³, ANNA PASQUALI⁴, DANIEL H. MCINTOSH^{5,3}, SIMONE M. WEINMANN⁶

Draft version May 29, 2019

ABSTRACT

Using dark matter halos traced by galaxy groups selected from the Sloan Digital Sky Survey Data Release 4, we find that about 1/4 of the faint galaxies ($^{0.1}M_r - 5 \log h > -17.05$, hereafter dwarfs) that are the central galaxies in their own halo are not blue and star forming, as expected in standard models of galaxy formation, but are red. Many red dwarf galaxies are physically associated with more massive halos. About $\sim 30\%$ of red dwarf galaxies reside in massive halos as satellites, while another $\sim 30\%$ has a spatial distribution that is much more concentrated towards their nearest massive haloes than other dwarf galaxies. We use mock catalogs to show that the reddest population of non-satellite dwarf galaxies are distributed within about 3 times the virial radii of their nearest massive halos. We suggest that this population of dwarf galaxies are hosted by low-mass halos that have passed through their massive neighbors, and that the same environmental effects that cause satellite galaxies to become red are also responsible for the red colors of this population of galaxies. We do not find any significant radial dependence of the population of dwarf galaxies with the highest concentrations, suggesting that the mechanisms operating on these galaxies affect color more than structure. However, over 40% of dwarf galaxies are red and isolated and their origin remains unknown.

Subject headings: dark matter - large-scale structure of the universe - galaxies: halos

1. INTRODUCTION

In the current paradigm of galaxy formation, it is believed that virtually all galaxies initially form as ‘disks’ owing to the cooling of gas with non-zero angular momentum in virialized dark matter haloes. This smooth gas accretion dominates the galactic gas supply and hence the fuel for star formation. Galaxies that reside in the centers of lower mass halos, those with masses less than $M_{\text{halo}} \lesssim 3 \times 10^{11} h^{-1} M_{\odot}$, accrete gas through very efficient cold mode accretion, i.e. gas that is never heated (Keres et al. 2005, Keres et al. 2008). The central galaxies that reside in larger halos accrete their gas through the classic, but less efficient, hot mode of accretion where the gas is shock heated to near the virial temperature near the virial radius and then must cool to be accreted by the central galaxy. Hence the naive expectation would be that dwarf galaxies should be actively star forming and blue.

However, when a small halo is accreted by a larger halo, i.e. when it becomes a subhalo, the central galaxy that formed in the small halo becomes a satellite galaxy and may experience a number of environmental effects that may change its properties. For instance, the diffuse gas originally associated with the subhalo may be

stripped, thus removing the fuel for future star-formation (e.g. Larson, Tinsley & Caldwell 1980). This process, referred to as strangulation (Balogh & Morris 2000), can result in a gradual decline of the star formation rate in the satellite galaxy, making it redder with the passage of time. If the external pressure is sufficiently high, ram-pressure stripping may also be able to remove the entire cold gas reservoir of the satellite (e.g. Gunn & Gott 1972), causing a fast quenching of its star formation. A satellite galaxy is also subject to tidal heating and stripping and galaxy harassment (Moore et al 1996), which may also cause the satellite to lose its fuel for star formation. These processes are believed to have played an important role in the evolution of satellite galaxies, and to be responsible, to a large extent, for the relation between galaxy properties and their environment. Indeed, satellite galaxies are generally found to be redder and somewhat more concentrated than central galaxies with similar stellar masses (e.g. van den Bosch et al. 2008a; Weinmann et al. 2008; Yang et al. 2008b; c).

Furthermore, recent investigations based on cosmological N -body simulations have shown that a significant fraction of dark matter haloes that are close to, but beyond the virial radius of, a more massive neighboring halo, are physically connected to their neighbor. As shown by Lin et al. (2003) and more recently by Ludlow et al. (2008), some low-mass halos are *physically* associated with more massive halos, in the sense that they were once subhalos within the virial radii of these more massive progenitors and have subsequently been ejected. This population of halos was found to extend beyond three times the virial radii of their host halos, and represents about 10% of the entire population of low-mass halos (Wang, Mo & Jing 2008). If galaxies have managed to form in the progenitors of these ejected halos, it is likely that the same environmental processes operating on satellite galaxies may also have affected the proper-

¹ Shanghai Astronomical Observatory, the Partner Group of MPA, Nandan Road 80, Shanghai 200030, China; E-mail: yuwang@shao.ac.cn

² Joint Institute for Galaxy and Cosmology (JOINGC) of Shanghai Astronomical Observatory and University of Science and Technology of China

³ Department of Astronomy, University of Massachusetts, Amherst MA 01003-9305

⁴ Max-Planck-Institute for Astronomy, Königstuhl 17, D-69117 Heidelberg, Germany

⁵ Department of Physics, 5110 Rockhill Road, University of Missouri at Kansas City, Kansas City, MO 64110

⁶ Max-Planck-Institut für Astrophysik, Karl-Schwarzschild-Strasse 1, 85748 Garching, Germany

ties of these galaxies. In particular, we would expect the presence of a red population of faint galaxies that are closely associated with massive halos that once hosted them.

Galaxies are observed to be bimodal in the color-magnitude plane: red galaxies with very little star formation (the red sequence) and blue star forming galaxies that are typically disk (the blue cloud) (e.g. Kauffman et al. 2003, Baldry et al. 2004). Extrapolating the observed division line (Yang et al. 2008a) to dwarf galaxies we surprisingly find that for central dwarf galaxies in the SDSS, with r -band magnitudes between -14.46 and -17.05, just over 1/4 are red. In this paper we will investigate the nature of these red dwarf galaxies. Quantifying the spatial distribution of this population of galaxies is clearly important, because it allows us to determine whether or not they can be explained as a population of satellite galaxies that were ejected from larger halos.

In this paper, we use the galaxy group catalogue constructed by Yang et al. (2007) from the Sloan Digital Sky Survey Data Release 4 (SDSS DR4; Adelman-McCarthy et al. 2006) to study the distribution of central dwarf galaxies around massive halos. The structure of this paper is as follows. In §2 we briefly describe the criteria used to select galaxies and galaxy groups. In §3 we study the radial distribution of dwarf galaxies around their nearest neighbor halos and its dependence on galaxy color and concentration. Some systematic effects that may change our results are discussed in §4. In §5, we use mock catalogues to test the reliability of our results and to quantify their implications. Finally, in §6, we present some further discussion regarding our results.

2. OBSERVATIONAL DATA

2.1. Samples of Galaxy Groups

Our analysis uses the galaxy group catalogues of Yang et al. (2007), which were constructed from the New York University Value-Added Galaxy Catalog (NYU-VAGC, see Blanton et al. 2005b) based on the Sloan Digital Sky Survey Data Release 4 (SDSS DR4; Adelman-McCarthy et al. 2006). Only galaxies in the Main Galaxy Sample with redshifts in the range $0.01 \leq z \leq 0.20$ and with a redshift completeness $\mathcal{C} > 0.7$ were used. Three sets of group catalogues were constructed using a modified version of an adaptive halo-based group finder, which was optimized to assign galaxies into groups according to their common dark matter halos (Yang et al. 2005). For our study here, we use group sample II, in which only galaxies with spectroscopic redshifts (either provided by the SDSS or taken from alternative surveys) are used. We have tested, though, that using group sample III, which also includes galaxies that have been missed owing to fiber collisions, does not have a significant impact on any of our results.

For each group in the catalogue, Yang et al. (2007) estimated the corresponding halo mass using either the ranking of its characteristic luminosity (this mass is denoted by M_L) or using the ranking of its stellar mass (this mass is denoted by M_S). Throughout this paper, we use M_S as our halo masses. We have also tested that using M_L instead does not change any of our results. As described in Yang et al. (2007), the characteristic luminosity and stellar mass of a group are defined to be

the total luminosity and total stellar mass of all group members, respectively, with $^{0.1}M_r - 5 \log h \leq -19.5$. Thus, groups whose member galaxies are all fainter than $^{0.1}M_r - 5 \log h = -19.5$ cannot be assigned halo masses according to the ranking. For these groups, the halo masses are estimated in the following way. In Yang et al. (2008b) it is shown that the stellar masses of central galaxies are tightly correlated with the masses of their host haloes. The mean of this relation is well described by

$$M_* = M_0 \frac{(M_h/M_1)^{\alpha+\beta}}{(1 + M_h/M_1)^\beta}, \quad (1)$$

where M_* and M_h are the central galaxy stellar mass and the host halo mass of the group, respectively, and $(\log M_0, \log M_1, \alpha, \beta) = (10.306, 11.040, 0.315, 4.543)$. For groups that cannot be assigned a halo mass according to the stellar-mass (luminosity) ranking, we use the above relation to obtain M_h through the stellar masses of their central galaxies.

2.2. Galaxy Samples

Group catalogue II consists of 369447 galaxies, which are assigned into 301237 groups. The majority, 271420, of the groups contain only one member, i.e., all of them are the central galaxies of the groups. The remaining 98027 galaxies are in groups with more than one member, and 29817 of them are *central* galaxies (the brightest one in each group). We refer to the other 68210 galaxies as *satellites* (Yang et al. 2007).

From our galaxy sample, we select three subsamples of dwarf galaxies as follows. We rank order all galaxies according to their absolute magnitudes (in the r -band, K - and evolution- corrected to redshift $z = 0.1$), starting with the faintest galaxy. The 1500 galaxies with the highest rank (i.e. the 1500 faintest galaxies) make up our first sample, called S1. The galaxies with ranks 1501-3000 make up sample S2, and those with ranks 3001-4500 sample S3. Table 1 lists the (sequential) absolute magnitude ranges of all three samples, as well as the numbers of central and satellite galaxies. Note that all the galaxies in S1, S2 and S3 are fainter than $^{0.1}M_r - 5 \log h = -17.05$. In what follows we refer to all galaxies in these three samples as dwarf galaxies.

To study how the spatial distribution of dwarf galaxies depends on galaxy color, we separate each of the samples, S1, S2, and S3, into red and blue subsamples. In particular, we define a color cut

$$^{0.1}(g-r) = a + b (^{0.1}M_r - 5 \log h), \quad (2)$$

and we adjust the parameters a and b such that samples S1, S2, and S3 roughly have the same fractions of galaxies, f_{red} , redder than this particular cut. We consider four values for f_{red} : 20%, 30%, 40%, and 50%, for which we obtain $[a, b] = [-0.421, -0.060]$, $[-0.423, -0.055]$, $[-0.375, -0.049]$ and $[-0.313, -0.043]$, respectively. Thus, if $f_{\text{red}} = 20\%$ it means that the red subsamples of S1, S2 and S3 each consist of the 20% reddest galaxies in their particular samples, etc. Fig 1 shows the color-magnitude relations of galaxies in S1, S2 and S3 (delineated by vertical dashed lines). The four panels correspond to the four different values of f_{red} , as indicated, and the solid line in each panel corresponds to the color cut of Eq. (2) used in each case.

TABLE 1
GALAXY SAMPLES

ID (1)	$^{0.1}M_r - 5 \log h$ (2)	N_{total} (3)	N_{cent} (4)	N_{sat} (5)	$f_{\text{red,cent}}$ (6)	$f_{\text{red,sat}}$ (7)	$f_{\text{red,cent}}^b$ (8)	$f^b(r_p/R_{180}) \leq 3$ (9)
S1	(-14.46,-16.36]	1500	1103	397	13.69%	37.53%	33.79%	34.60%
S2	(-16.36,-16.78]	1500	1081	419	13.69%	36.28%	22.50%	47.46%
S3	(-16.78,-17.05]	1500	1008	492	10.20%	40.24%	19.51%	47.72%
S1+S2+S3	(-14.46,-17.05]	4500	3192	1308	12.59%	38.15%	25.49%	41.63%
S4		1500	1080	420	13.51%	37.02%		

NOTE. — Column 1 indicates the sample ID. Column 2 lists the absolute magnitude range of each sample. Columns 3 to 5, indicate the number of total, central and satellite galaxies in each sample, respectively. Columns 6 and 7 list the red fractions among central and satellite galaxies, respectively, where the red galaxies are defined to be the reddest 20% of all the galaxies. Column 8 lists the red fraction of central dwarf galaxies where the red galaxies are defined by extrapolating the division between red sequence and blue cloud galaxies from Yang et al. (2008a). Column 9 lists the fraction of these (in Column 8) central red dwarf galaxies that have $r_p/R_{180} \leq 3$.

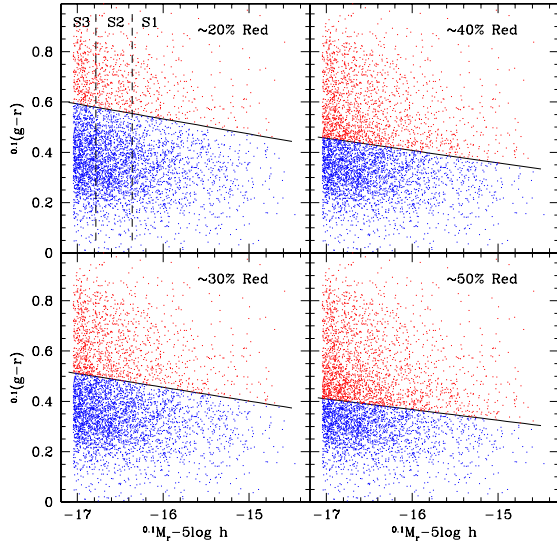


FIG. 1.— The color-magnitude distribution of dwarf galaxies (including central and satellite galaxies). In four panels the dwarf galaxies are separated into 20%, 30%, 40%, 50% red galaxies as indicated, respectively. The vertical dashed lines in the upper-left panel show the separation criteria of samples S1, S2 and S3.

In Table 1 we list, for each sample, the red fractions of central ($f_{\text{red,cent}}$) and satellite galaxies ($f_{\text{red,sat}}$). Here red galaxies are defined to be the reddest 20% of all galaxies (both centrals and satellites) in our sample of dwarf galaxies. Clearly, dwarf galaxies that are satellites have a much higher red fraction than central dwarf galaxies. For comparison, extrapolating the observed division line between the red sequence and the blue cloud from Yang et al. (2008a) down to dwarf galaxies one would find that 33.8%, 22.5%, and 19.5% of the central galaxies in the S1, S2, and S3 samples, respectively, were red.

3. THE DISTRIBUTION OF CENTRAL DWARFS

In this section, we investigate how central dwarf galaxies are distributed with respect to their nearest more massive halo (i.e. more massive than their own halo). Since the distances of galaxies based on redshifts suffer from redshift distortions, we separate the distance between a central dwarf galaxy and its nearest more massive halo into two components: π , which is the separation along the line-of-sight, and r_p , which is the separation in the perpendicular direction.

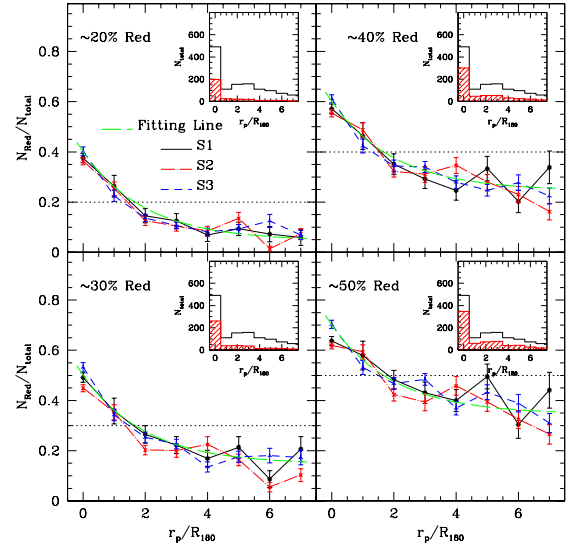


FIG. 2.— Fractions of the red central galaxies near more massive halos as a function of projected distance r_p/R_{180} . The four panels show the results of the color subsamples with 20%, 30%, 40% and 50% red galaxies, respectively. The related color subsample separation criteria are shown in Fig. 1. The different lines correspond to the different samples as indicated. The fit long-dashed, green line is described in the text. For comparison, we show the fraction of red *satellite* galaxies that are within the same luminosity ranges as the central galaxies at $r_p/R_{180} = 0$. The small window within each panel shows the number counts of dwarf central (or satellite) galaxies in S1 as a function of r_p/R_{180} : black histogram for all galaxies and shaded, red histogram for red galaxies.

For each group in the catalogue, we use the assigned halo mass, M_S , to estimate its halo radius, $R_{180} = [3M_S/(4\pi * 180\bar{\rho})]^{1/3}$, which follows from defining the mean mass density within a halo as 180 times the average density of the universe, $\bar{\rho}$. We search around each central dwarf galaxy, within a line-of-sight separation $|\pi| = 15 h^{-1}\text{Mpc}$,⁷ for the group that has (i) a halo mass larger than that of the dwarf galaxy in question and (ii) the lowest value of r_p/R_{180} (with R_{180} the halo radius of the group). The central galaxy is then said to be at a scaled ‘distance’ r_p/R_{180} from a massive halo, and the halo is referred to as the nearest halo of the

⁷ Tests have shown that changing the line-of-sight separation for the search from $|\pi| \leq 15 h^{-1}\text{Mpc}$ to $|\pi| \leq 10 h^{-1}\text{Mpc}$ or to $|\pi| \leq 20 h^{-1}\text{Mpc}$ does not have a significant impact on any of our results.

galaxy. We use this scaled distance because R_{180} is the only important length scale related to the dynamics of a virialized halo.

3.1. Color Dependence

Fig. 2 shows the fraction $N_{\text{red}}/N_{\text{total}}$ of central dwarf galaxies that are red as a function of the scaled distance, r_p/R_{180} , to their nearest halos. Here N_{total} is the total number of dwarf galaxies in each sample (S1, S2 or S3) in that bin of r_p/R_{180} , and N_{red} is the number of those galaxies that are red according to the criterion used. The numbers are shown in the small window in each panel (the black histogram for N_{total} , and the red, hatched histogram for N_{red}). The four panels show the results for $f_{\text{red}} = 20\%$, 30% , 40% and 50% . In each panel, the different lines show the results obtained for the three samples, S1, S2, and S3, as indicated in the upper-left panel. The error-bars are obtained using 100 bootstrap resamplings (Barrow, Bhavsar, & Sonoda 1984; Mo, Jing & Börner 1992). Galaxies are counted in bins specified by $N - 0.5 \leq r_p/R_{180} \leq N + 0.5$ (for $N = 2, 3, \dots, 7$), and $0 \leq r_p/R_{180} \leq N + 0.5$ for $N = 1$. For comparison, the data point at $r_p/R_{180} = 0$, indicates the fraction of red *satellite* galaxies within the same luminosity range as the central galaxies. Note that the results obtained for S1, S2, and S3 are almost identical, indicating that the spatial distribution of dwarf galaxies around massive haloes does not depend on their luminosities. However, if we consider much brighter galaxies, e.g. at $^{0.1}M_r - 5 \log h \sim -18.5$, the radial dependence starts to level off.

There is a clear trend that the fraction of red central dwarf galaxies increases with decreasing scaled distance to the nearest halo. The fraction of the 20% reddest population at $r_p/R_{180} \gtrsim 4$ is around 5% to 10%, increases systematically to $\sim 25\%$ at $r_p/R_{180} \sim 1$, and to $\sim 40\%$ at $r_p/R_{180} = 0$ for the satellite galaxies. For the other three cases (with $f_{\text{red}} = 30\%$, 40% and 50%), the fraction also decreases with r_p/R_{180} , but reaches a higher level at large r_p/R_{180} . This indicates that the less red galaxies in these subsamples are not strongly associated with massive halos. We quantify the association of red dwarf galaxies with massive halos by fitting the data obtained from S3 shown in the four panels simultaneously with a function $f = a + b \times \exp(-x/2)$, where $x = r_p/R_{180}$. In the fit we subtract a constant of, 0.1, 0.2 and 0.3, from the data for the 30%, 40% and 50% reddest subsamples, respectively, to account for the component that is not closely associated with massive halos. The best fit results, with $a = 0.045$ and $b = 0.356$, are shown in each panel of Fig. 2 as the green, long-dashed lines. We have also checked the radial distribution of the central dwarf galaxies when using $f_{\text{red}} = 15\%$ to define the subsample of red dwarfs. In this case, we find less than a 5% decrease in the red fraction at large r_p/R_{180} , indicating that the 5% least red galaxies in the 20% reddest subsample are not randomly distributed relative to the massive halos. Thus the overall results suggest that the 15% - 20% reddest dwarf galaxies are quite distinct from the other dwarfs, in that they reveal a clear preference to reside close to their nearest more massive dark matter halo. In §5, we use mock galaxy redshift surveys constructed from cosmological N -body simulations to quantify this connection.

3.2. Concentration Dependence

Apart from a color dependence, we also check whether the radial distribution of dwarf galaxies with respect to their nearest more massive dark matter halos depends on their surface brightness profiles. To this end, we split our dwarf galaxies into two subsamples according to the value of their concentration parameter $C = r_{90}/r_{50}$. Here r_{90} and r_{50} are the radii that contain 90 and 50 percent of the Petrosian r -band flux, respectively. As shown in Strateva et al. (2001), C is a reasonable proxy for the Hubble type, with $C > 2.6$ corresponding to early-type galaxies. We, therefore, separate galaxies into high ($C > 2.6$) and low ($C \leq 2.6$) concentrations, as illustrated in the lower-right panel of Fig. 3. Roughly 20% of the dwarf galaxies thus end up in the high-concentration subsample.

The lower-right panel of Fig. 4 shows the fraction of galaxies in this high-concentration subsample as a function of the scaled distance to the nearest more massive halo. Unlike the reddest galaxies, the most concentrated galaxies have a radial distribution that is similar to that of the total population of central dwarf galaxies. Note however, for brighter galaxies, especially in and around clusters, there is a so called morphology-radius relation (e.g., Dressler et al. 1997), which according to Park & Hwang (2008) may be largely induced by the interaction of the target galaxy with its nearest (early-type) neighbor galaxy.

4. SYSTEMATICS

Before we proceed to study the origin of the central red dwarf galaxies, there are a number of issues that need to be addressed. An obvious worry is that the group finder is not perfect, and has misclassified a number of satellite galaxies as central galaxies. We will discuss this issue in more detail with the help of mock galaxy and group catalogs in §5. In this section we discuss systematics that can be addressed without the need for mock catalogs.

4.1. Stellar Mass Dependence

For a given luminosity, redder galaxies are expected to have a larger stellar mass. The color separation used above may thus introduce a bias in the sense that galaxies in the redder subsample are systematically more massive. To check whether or not the color distribution we obtained in the previous section is robust when the dwarf galaxies are selected in a similar stellar mass bin, we construct a controlled subsample S4. Note that the survey *magnitude limit* of the SDSS observation corresponds to a higher (lower) *stellar mass limit* for the redder (bluer) galaxies. In general, one can construct a stellar mass limit sample (and hence the subsample S4) for all (including both red and blue) galaxies by adopting the stellar mass limit (as a function of redshift) for the reddest galaxies (see Appendix of van den Bosch et al. 2008b), which, however, may significantly reduce the number of dwarf galaxies in our sample. Instead, as a rough approximation, we construct subsample S4 as follows (with the hidden assumption that if the galaxies are complete in both luminosity and stellar mass they have similar color distributions and thus similar red and blue fractions). First, we separate all the dwarf galaxies into red and blue populations: the reddest 20% being red and the rest being blue, using the separation line shown in

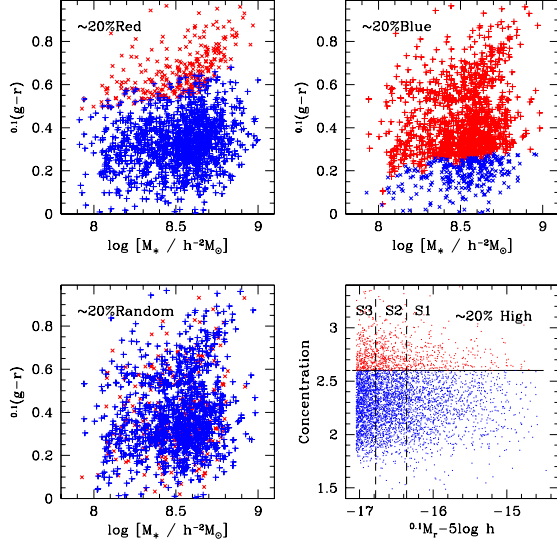


FIG. 3.— Upper-left panel: the color-stellar mass distribution of the 20% red (‘x’-crosses) and 80% blue (‘+’-crosses) dwarf galaxies in terms of *similar stellar masses*. Upper-right panel: the same set of dwarf galaxies as in the upper-left panel, but separated into 20% blue (‘x’-crosses) and 80% red (‘+’-crosses). Lower-left panel: the same set of dwarf galaxies as in the upper-left panel, but randomly selected and separated into 20% (‘x’-crosses) and 80% (‘+’-crosses) populations. Lower-right panel: the concentration-magnitude distribution of the dwarf galaxies, which are separated into $\sim 20\%$ high and $\sim 80\%$ low concentration populations by $C = 2.6$.

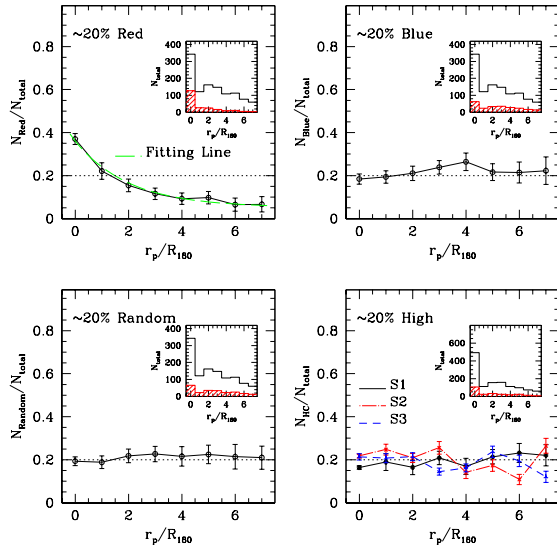


FIG. 4.— Similar to Fig. 2, but with related subsample separation criteria shown in Fig. 3. Upper-left panel: fraction of the red central galaxies near more massive halos as a function of r_p/R_{180} , where the 20% red population is defined with respect to the similar stellar mass galaxies. Upper-right panel: similar to the upper-left panel but for the 20% blue population. Lower-left panel: similar to the upper-left panel but for the 20% random population. Lower-right panel: fraction of the high concentration $C > 2.6$ central galaxies near more massive halos as a function of r_p/R_{180} .

the upper-left panel of Fig. 1. Next, for each of the $(1500 \times 20\% = 300)$ red galaxies in S1, we randomly select four blue galaxies from the blue population with stellar masses within $\Delta \log M_* = 0.025$ of the red galaxy. This yields a blue control sample of $(1500 \times 80\% = 1200)$ dwarf galaxies, which has the same stellar mass distribution as the 20% reddest galaxies. The control subsample S4 so constructed has exactly the same red fraction of dwarf

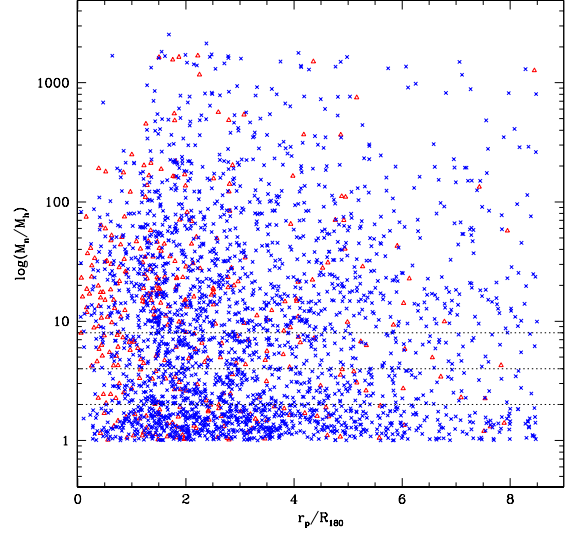


FIG. 5.— The nearest neighbor to host halo mass ratio M_n/M_h - projected distance r_p/R_{180} distribution of the dwarf central galaxies in samples S1+S2+S3. The triangles and crosses show the red and blue central galaxies, respectively, where the red population is defined to be the 20% reddest all galaxies.

galaxies as S1, but now with respect to blue galaxies with similar stellar masses. The upper-left panel of Fig. 3 shows the color-stellar mass relation for S4, split into red and blue galaxies.

For comparison, we also form the following two subsamples from S4. In one, we randomly select 20% of the galaxies from S4; in the other, we select the 20% bluest galaxies that have the same stellar mass distribution as all the galaxies in sample S4. The color-stellar mass relations of these two subsamples are shown in the lower-left and upper-right panels of Fig. 3, respectively.

The upper-left panel of Fig. 4 shows $N_{\text{red}}/N_{\text{total}}$ as a function of r_p/R_{180} obtained using sample S4. Fitting the data again with the function $f = a + b \times \exp(-x/2)$, we obtain $a = 0.053$ and $b = 0.309$, and the corresponding model is shown as the long-dashed curve. This dependence on the scaled distance, $x \equiv r_p/R_{180}$, is only slightly weaker than that for the corresponding luminosity sample S1, indicating that the bias caused by the stellar-mass difference between the red and blue subsamples is not important.

The upper-right and lower-left panels of Fig. 4 show the results obtained for the 20% bluest galaxies and for the 20% random galaxies (as defined above). For these two cases there is no significant radial dependence. Although one expects such a lack of radial dependence for the random subsample, it does indicate that there are no significant systematic errors in our analysis. The lack of a radial dependence for the 20% bluest subsample is due to the fact that only the $\sim 15 - 20\%$ reddest galaxies reveal a radial distribution that is peaked towards smaller r_p/R_{180} .

4.2. Dependence on the Mass of the Nearest Neighbor

In our analysis above, the “nearest more massive halo” of a central dwarf galaxy is defined as the halo with a line-of-sight separation $|\pi| \leq 15 h^{-1} \text{Mpc}$ which has (i) a mass that is more massive than that of the dwarf galaxy, and (ii) the smallest value of r_p/R_{180} (see section 3). This implies that some of these nearest more massive halos

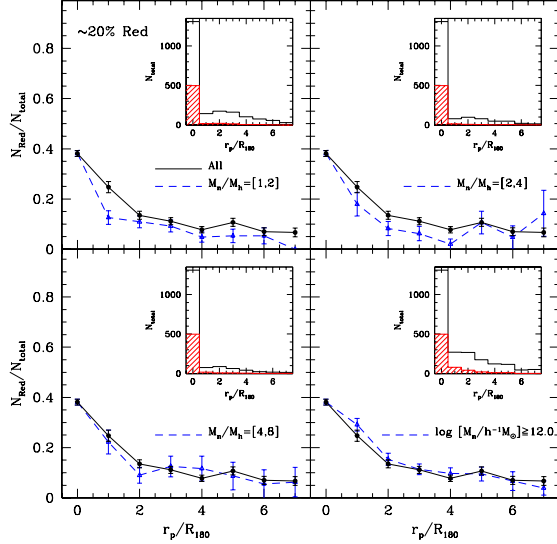


FIG. 6.— Similar to Fig. 2, but for all galaxies in samples S1+S2+S3 within different central-nearest halo systems. In each panel the selection criteria, M_n/M_h , is indicated. Here the results are shown for the fraction of the 20% red population. For comparison, in each panel, we also show as the symbols with solid line the results for all central-nearest halo systems.

may have masses that are only slightly larger than that of the dwarf galaxy under consideration.

In what follows we use M_h to refer to the halo mass of the central dwarf galaxy, and M_n to refer to the mass of its nearest more massive halo. For our combined sample (S1 + S2 + S3) the average value of M_h is about $10^{10.9} h^{-1} M_\odot$. Fig. 5 shows the ratio M_n/M_h as a function of the scaled distance r_p/R_{180} for all central dwarf galaxies in S1+S2+S3. Here the results for the 20% reddest galaxies are shown as red triangles, while the other 80% are indicated by blue crosses. Note that there is a very large amount of scatter in M_n/M_h , ranging from unity to well in excess of 1000.

It is interesting to investigate whether the color dependence of the radial distribution of central dwarfs with respect to their nearest more massive halo depends on M_n . This can provide valuable insight into the actual origin of this color dependence. We therefore proceed as follows. We first combine samples S1+S2+S3, and then calculate the fraction of central red dwarf galaxies that belong to the 20% reddest subsample as we did in §3. However, now we only select systems for which M_n/M_h is restricted to [1,2], [2,4], [4,8] or $\log[M_n/h^{-1} M_\odot] \geq 12.0$, respectively. The results are shown in the four panels of Fig. 6 as indicated. For comparison we also show, in each panel, the results obtained for all systems (i.e. $M_n/M_h > 1$). A comparison of all four panels shows that there is a clear, albeit somewhat weak, dependence of the trend on M_n/M_h . Overall, the colors of central dwarf galaxies are most strongly affected by nearest neighbor halos that are more massive. In the case of $1 < M_n/M_h \leq 2$ (upper-left panel), the central dwarf galaxies have a $N_{\text{red}}/N_{\text{total}}$ that is almost independent of r_p/R_{180} , and much lower than that of the dwarf satellites. On the other hand, the central dwarfs that are distributed around halos more massive than $10^{12.0} h^{-1} M_\odot$ (lower-right panel), have a radial dependence that is somewhat stronger than that for all systems.

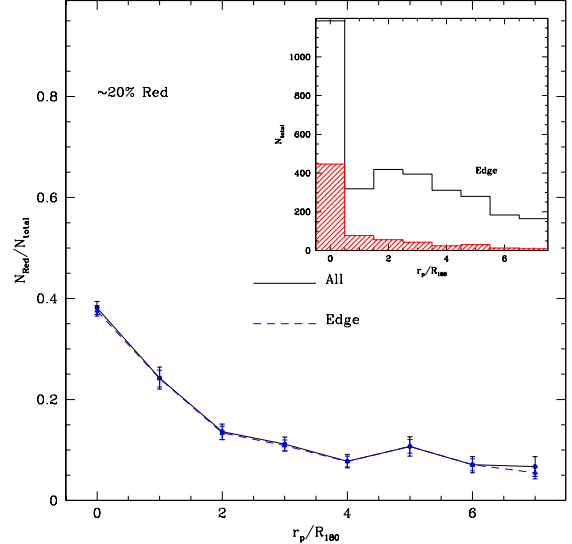


FIG. 7.— Similar to Fig. 2, but here we compare the results for all galaxies in samples S1+S2+S3, with and without edge effects by removing the central dwarf galaxies that are near the survey edge.

4.3. Survey Edge Effect

Since the SDSS is not a full-sky survey, and since our group catalogue is constructed using only galaxies with redshifts $0.01 \leq z \leq 0.2$, our results may be influenced by edge effects of the survey: for central dwarf galaxies near an edge of the survey, there is an enhanced probability that it is actually a satellite (or central) galaxy in a more massive group (halo), but for which all other members just happen to lie beyond the edges of the survey. Although we tried to take these effects into account when assigning halo masses to our groups (see Yang et al. 2007 for details), it could still be that a significant fraction of our central dwarf galaxies are in reality misclassified centrals or satellites owes to the survey geometry.

To check the impact of these edge effects, we follow Yang et al. (2007) by measuring the edge parameter f_{edge} . For each central dwarf galaxy in S1+S2+S3, we randomly distribute 500 points within a radius $1 h^{-1} \text{Mpc}$. Next we apply the SDSS DR4 survey mask and remove those random points that fall outside of the region where the completeness $\mathcal{C} > 0.7$. For each central dwarf galaxy we then compute the number of remaining points, N_{remain} , and we define $f_{\text{edge}} = N_{\text{remain}}/500$ as a measure for the volume around the central dwarf galaxy that lies within the survey edges. To test the impact of edge effects on our measurements in §3, we remove those central dwarf galaxies with $f_{\text{edge}} \leq 0.8$ (about 13%) and recalculate the radial distribution of the remaining central galaxies. The result is shown in Fig. 7 (dashed line), compared to the results for all the central dwarfs, independent of their value of f_{edge} (solid line). Clearly, the two curves are almost indistinguishable, indicating that our results are not an artifact of survey edge effects.

5. TEST WITH MOCK SAMPLES

One potential problem with the results presented above is that the group finder used to identify galaxy groups is not perfect. Hence, some of the dwarf galaxies classified as central galaxies may in fact be satellite galaxies. To test the severity of such effects and to quantify

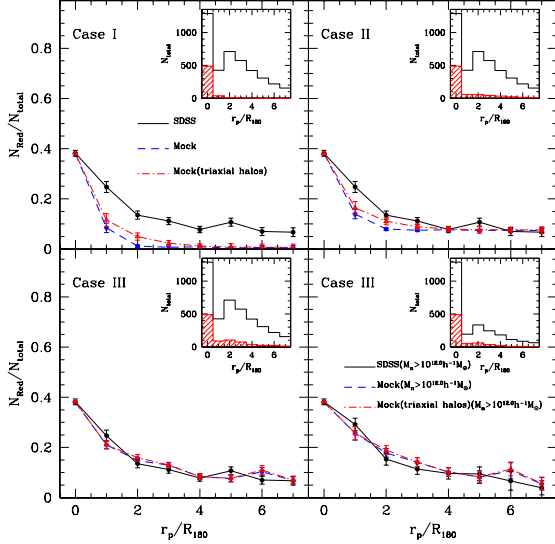


FIG. 8.— Similar to Fig. 2, but here we compare the observational and mock results. The upper-left, upper-right and lower-left panels show the results for all host-nearest halo systems using different color models: Case I, II and III as indicated (see text). In the lower-right panel, we show results for those central-nearest halo systems with $M_n \geq 10^{12.0} h^{-1} M_\odot$ using color model Case III but with different parameters. In each panel, the symbols connected with dashed lines are results obtained from the mock galaxy and group catalogues where the halos are assumed to be spherical. The symbols connected with dot-dashed lines are results obtained from the mock galaxy and group catalogues where the halos are assumed to follow a triaxial Jing & Suto (2002) profile. For reference, in each panel we also show, as the dots connected with solid lines, the results we obtained for the SDSS samples S1+S2+S3. See text for details.

the true association between central dwarf galaxies and their nearby massive halos, we apply the same analysis to mock samples and compare the results with the observational data that we have obtained. Here we use the mock SDSS DR4 galaxy and group catalogues that are constructed by Yang et al. (2007) to test the performance of the group finder. Following Yang et al. (2004), the mock galaxy catalogue is constructed by populating dark matter haloes in numerical simulations of the standard Λ CDM model with galaxies of different luminosities, using the conditional luminosity function (CLF) model of Cacciato et al. (2008). This CLF describes the halo occupation statistics of SDSS galaxies, and accurately matches the SDSS luminosity function, as well as the clustering and galaxy-galaxy lensing data of SDSS galaxies as a function of their luminosity. Next a mock redshift survey is constructed mimicking the sky coverage of the SDSS DR4 and taking detailed account of the angular variations in the magnitude limits and completeness of the data (see Li et al. 2007 for details). Finally we construct a group catalogue from this mock redshift survey, using the same halo-based group finder as for the real SDSS DR4.

To test the impact of contamination on our observational results obtained above, we consider three models for the distribution of red dwarf galaxies:

- Case I: Here we assume that a fraction, $f_{\text{red,sat}}$, of true *satellite* dwarf galaxies are red, but that all true central dwarf galaxies are blue.
- Case II: Same as Case I, but here we assume that a fraction, $f_{\text{red,cent}}$, of true central dwarf galaxies

are also red and have the same spatial distribution as blue central dwarfs.

- Case III: Similar to Case II, but here we assume that $f_{\text{red,cent}}$ depends on the distance of the central galaxy to its nearest more massive halo, according to $f_{\text{red,cent}}(r) = a + b \times \exp(-(y-1)/2)$. Here a and b are constants and $y = r/R_{180}$.

These models are used to assign a color to each of the mock dwarf galaxies according to their positions in real space and their true membership of host halos.

As for the observational data, we select the 4500 faintest galaxies from the mock group catalogue, using the same criteria as described in Subsection 2.2. We choose the observational result for the central galaxies in S1+S2+S3 (shown as the dots with error bars in Fig. 6 to compare with our models. As discussed in the previous section, this result is representative of the distribution of red dwarf galaxies with respect to their nearest more massive halos. For all Cases (I, II and III), we adopt $f_{\text{red,sat}} = 0.38$ so that the red fraction of the satellite galaxies is consistent with the SDSS data (repeated in Fig. 8 as a solid line). In Case II we set $f_{\text{red,cent}} = 0.07$, so that the red fraction of the central galaxies at large projected distance, $r_p/R_{180} \geq 4$, is roughly the same as the observational data. The corresponding results obtained from Case I and Case II are shown in the upper-left and upper-right panels of Fig. 8, respectively. It is clear that in Case I, in which the only red dwarfs are satellites, the fraction of false central galaxies in the mock catalogue is too small to match the observational data at $r_p/R_{180} \gtrsim 1$. For Case II, although by construction the fraction of red central galaxies matches the observational results at large $r_p/R_{180} \geq 4$, the model underestimates the fraction of red central galaxies at intermediate r_p/R_{180} . These results indicate that (i) not all red dwarf galaxies are satellites, and (ii) the central red dwarf galaxies have a different distribution than the total central dwarf population.

Now, let us look at Case III. We have experimented with different values for a and b , and found that the following set of parameters matches the observational data reasonably well: $(a, b) = (0.05, 0.36)$. The results obtained from the mock catalogue using this set of model parameters are shown in the lower-left panel of Fig. 8. This shows that the central red dwarf galaxies are correlated with massive halos on scales given by $(y-1) \lesssim 2$ (i.e. $r \lesssim 3R_{180}$).

Finally, as we did for the observational sample, we can also obtain $f_{\text{red,cent}}(r)$ for dwarf galaxies near halos of different masses using the mock sample Case III. As an illustration, we consider the case with $M_n \geq 10^{12.0} h^{-1} M_\odot$. The model for $f_{\text{red,cent}}(r)$ that best matches the observational result has $(a, b) = (0.05, 0.45)$ and is slightly steeper than that obtained for the case without any restrictions on M_n . The model prediction obtained from the mock sample is shown in the lower-right panel of Fig. 8 along with the corresponding observational data.

In the mock catalogue considered above, the distribution of satellite galaxies in individual halos is assumed to be spherically symmetric and to follow the NFW (Navarro, Frenk & White 1997) profile (see Yang et al. 2004 for details). In reality, the distribution of satellite galaxies in individual halos may not be spherical,

which may cause further contaminations of the group memberships selected by the group finder. To test this, we have constructed a mock catalogue assuming that the distribution of satellite galaxies in individual halos is triaxial, with axis ratios given by the model of Jing & Suto (2002) for CDM halos. We found a slightly higher level of contamination in this new mock catalogue, but it does not change any of our results significantly. As an illustration, in each panel of Fig. 8 we also show the results for non-spherical halos using symbols connected with dot-dashed lines. We obtain for Case III slightly weaker radial dependence with $(a, b) = (0.05, 0.34)$ and $(a, b) = (0.05, 0.43)$, for the cases shown in the lower-left and lower-right panels, respectively.

6. DISCUSSION

We set out to understand why about 1/4 of *central* dwarf galaxies, those with r -band magnitudes between -14.46 and -17.05, are red when one defines a dwarf galaxy to be red by extrapolating the division between red sequence galaxies and the blue cloud, as determined by Yang et al. (2008a) for brighter galaxies, down to dwarf magnitudes. Current models of galaxy formation would naively expect such galaxies to be blue since they would be efficiently accreting gas through cold mode accretion and rapidly converting it into stars.

In a recent study, Ludlow et al. (2008; see also Lin et al. 2003) analysed the properties of subhalos in galaxy-sized cold dark matter halos using a suite of cosmological N-body simulations. The subhalos in their definition refer to the whole population of subhalos physically associated with the main system, including both subhalos that are found within the virial radius of the host halo at the present time, and halos that were once within the virial radius of the main progenitor of the host and have survived as self-bound entities until $z = 0$. They found that such populations can extend beyond *three times* the virial radius, and contain objects on extreme orbits, with some approaching the nominal escape speed from the system. On average the subhalos identified within the virial radius represent only about *one half* of all associated subhalos, and many relatively central halos may have actually been ejected in the past from a more massive system. Since galaxies are assumed to form in dark matter halos, it is interesting to see if the results we obtain here can be understood in terms of galaxy formation in this population of subhalos.

According to the current theory of galaxy formation, satellite galaxies can experience various environmental effects that can quench their star formation and make them red (e.g., van den Bosch et al. 2008b and references therein). Because the galaxies in ejected subhalos have also been satellite galaxies, at least for some period of time, they are likely to have been subjected to similar environmental effects, and thus to have experienced some quenching of their star formation rates. It is thus likely that the association of red dwarf galaxies with massive halos presented here is produced by the association of ejected subhalos with their (former) hosts.

As shown in Table 1, about 30% of the dwarf galaxies are satellite galaxies. According to the results obtained by Ludlow et al. (2008), there should thus also be $\sim 30\%$ dwarf galaxies that are physically associated with nearby more massive halos out to about three times the virial

radius. If these associated galaxies (now outside their hosts) have properties similar to the satellite galaxies, we would expect a similar fraction of red dwarf galaxies that are distributed outside massive halos. This is qualitatively consistent with our findings presented above as shown in Table 1. However, since the observational data are obtained in redshift space and based on galaxy groups that may contain interlopers and may be incomplete, a detailed comparison between the data and the models requires the construction of mock catalogues that make use of the subhalo population and contain all the observational selection effects.

The fact that central dwarf galaxies have concentrations that are independent of their distances to the nearest massive halos indicates that the processes that causes them to become red does not have a significant impact on their structure. This is similar to the results obtained by van den Bosch et al. (2008a) who found that the transformation mechanisms operating on satellites affect color more than structure (see also Kauffmann et al. 2004; Blanton et al. 2005a; Ball, Loveday & Brunner 2008; Weinmann et al. 2008). Once again, this similarity between red dwarfs that are satellites and those that are centrals suggests that both populations may have experienced similar kinds of environmental effects.

However, as shown in Table 1, in the S1+S2+S3 sample less than 42% of the red dwarf central galaxies have $r_p/R_{180} \leq 3$. In other words, more than 58% of the red dwarf central galaxies are not close enough to a larger halo so that they could have been preprocessed there, becoming red and then subsequently being ejected. The origin of this population of central red dwarf galaxies, which is almost 15% of the combined S1+S2+S3 dwarf sample, still remains a mystery within the standard paradigm of galaxy formation. Furthermore, if we had used stellar mass instead of r -band magnitude to define our dwarf sample, the percentage of galaxies in this population would likely increase. This population of isolated red dwarfs are not merely a dust reddened star forming population seen near edge-on because their axis ratios are consistent with a randomly oriented population.

An outstanding problem for all galaxy formation models concerns the low mass slope of the galaxy mass function. CDM models in general predict too many low-mass dark matter haloes compared to the number of low mass galaxies. The mass function of dark matter haloes, $n(M)$, scales with halo mass roughly as $n(M) \propto M^{-2}$ at the low-mass end. This is in strong contrast with the observed luminosity function of galaxies, $\Phi(L)$, which has a rather shallow shape at the faint end, with $\Phi(L) \propto L^{-1}$. To reconcile this difference one usually invokes some form of feedback within these low mass halos. If the feedback mechanism were to prevent gas from entering these halos at late times, such galaxies would appear red. For example, the preheating mechanism of Mo et al. (2005), where gas is preheated by gas shocks within the forming large scale structures in which the low mass dark matter halos themselves are forming, has this feature. Therefore, this population of isolated, red, central dwarf galaxies could represent the tail of the process that prevents the vast majority of low mass dark matter halos from forming galaxies and their further study could shed new light on the mechanism responsible.

YW acknowledges the support of China Postdoctoral Science Foundation. This work is supported by the *One Hundred Talents* project, Shanghai Pujiang Program (No. 07pj14102), 973 Program (No. 2007CB815402), the CAS Knowledge Innovation Program (Grant No. KJXC2-YW-T05) and grants from

NSFC (Nos. 10533030, 10673023, 10821302). HJM would like to acknowledge the support of NSF AST-0607535, NASA AISR-126270 and NSF IIS-0611948. NSK would like to acknowledge the support of NASA LTSA NAG5-13102.

REFERENCES

- Adelman-McCarthy J.K., et al., 2006, *ApJS*, 162, 38
 Baldry I.K., Glazebrook K., Brinkmann J., Ivezić Z., Lupton R.H., Nichol R.C., Szalay A.S., 2004, *ApJ*, 600, 681
 Ball N.M., Loveday J., Brunner R.J., 2008, *MNRAS*, 383, 907
 Balogh M.L., Morris S.L., 2000, *MNRAS*, 318, 703
 Balogh M.L., Navarro J.F., Morris S.L., 2000, *ApJ*, 540, 113
 Barrow, J. D., Bhavsar, S. P., Sonoda, D. H., 1984, *MNRAS*, 210, 19
 Benson, A. J., 2005, *MNRAS*, 358, 551
 Blanton M.R., Eisenstein D.J., Hogg D.W., Schlegel D.J., Brinkmann J., 2005a, *ApJ*, 629, 143
 Blanton M.R. et al. , 2005b, *AJ*, 129, 2562
 Cacciato M., van den Bosch F. C., More S., Li R., Mo H. J., Yang X., 2008, preprint, arXiv:0807.4932
 Diemand, J., Kuhlen, M. Madau, P., 2007, *ApJ*, 657, 262
 Diemand, J., Kuhlen, M. Madau, P., 2007, *ApJ*, 667, 859
 Dressler A., et al., 1997, *ApJ*, 490, 577
 Gao, L., White, S.D.M., Jenkins, A., Stoehr, F., Springel, S., 2004, *MNRAS*, 355, 819G
 Ghigna, S., Moore, B., Governato, F., Lake, G. Quinn, T., Stadel, J., 1998, *MNRAS* 300, 146
 Ghigna, S., Moore, B., Governato, F., Lake, G. Quinn, T., Stadel, J., 1999, *aspc* 176, 140
 Giocoli C., Tormen G., van den Bosch F.C., 2008, *MNRAS*, 386, 2135
 Gunn J.E., Gott J.R., 1972, *ApJ*, 176, 1
 Jing Y.P., Suto Y., 2002, *ApJ*, 574, 538 (JS02)
 Kauffmann G., White S.D.M., Guiderdoni B., 1993, *MNRAS*, 264, 201
 Kauffmann G., Heckman T.M., White S.D.M., Charlot S., Tremonti, C., Peng E.W., Seibert M., Brinkmann J., Nichol R.C., SubbaRoa M., York D., 2003, *MNRAS*, 341, 54
 Kauffmann G., White S.D.M., Heckman T.M., Ménard B., Brinchmann J., Tremonti C., Brinkmann J., 2004, *MNRAS*, 353, 713
 Keres, D., Katz, N., Weinberg, D.H., & Daveé, R., 2005, *MNRAS*, 363, 2
 Keres, D., Katz, N., Fardal, M., Daveé, R., & Weinberg, D.H., 2008, *MNRAS*, submitted (arXiv:0809.1430)
 Larson R.B., Tinsley B.M., Caldwell C.N., 1980, *ApJ*, 237, 692
 Li C., Kauffmann G., Jing Y.P., White S.D.M., Börner G., Cheng F.Z., 2006, *MNRAS*, 368, 21
 Li C., Jing Y.P., Kauffmann G., Börner G., Kang X., Wang L., 2007, *MNRAS*, 376, 984
 Lin W.P., Jing Y.P., Lin L., 2003, *MNRAS*, 344, 1327
 Ludlow A.D., Navarro J.F., Springel V., Jenkins A., Frenk C.S., Helmi A., 2008, preprint, arXiv:0801.1127
 Mo H. J., Jing Y.P., Börner G., 1992, *ApJ*, 392, 452
 Mo H. J., Yang X., van den Bosch F.C., Katz N., 2005, *MNRAS*, 363, 1155
 Moore, B., Katz, N., Lake, G., Dressler, A. & Oemler, A., 1996, *Nature*, 379, 613
 Moore, B., Ghigna, S., Governato, F., Lake, G., Quinn, T., Stadel, J., Tozzi, P., 1999, *ApJ*, 524, L19
 Navarro J.F., Frenk C.S., White S.D.M., 1997, *ApJ*, 490, 493
 Park C., Hwang H.S., 2008, preprint, arXiv:0812.2088
 Quilis V., Moore B., Bower R., 2000, *Science*, 288, 1617
 Strateva I., et al., 2001, *AJ*, 122, 1861
 van den Bosch F.C., Tormen G., Giocoli C., 2005, *MNRAS*, 359, 1029
 van den Bosch F. C., Pasquali, A., Yang X., Mo H. J., Weinmann S.M., McIntosh D. H.; Aquino D., 2008a, preprint, arXiv:0805.0002
 van den Bosch F.C., Aquino D., Yang X., Mo H.J., Pasquali A., McIntosh D.H., Weinmann S.M., Kang X., 2008b, *MNRAS*, 387, 79
 Wang H. Y., Mo H. J., Jing Y. P., 2008, preprint, arXiv:0811.3558
 Weinmann S. M., Kauffmann G., van den Bosch F. C., Pasquali A., McIntosh D. H., Mo H., Yang X., Guo Y., 2008, preprint, arXiv:0809.2283
 Yang X., Mo H.J., Jing Y.P., van den Bosch F.C., Chu Y.Q., 2004, *MNRAS*, 350, 1153
 Yang X., Mo H.J., van den Bosch F.C., Jing Y.P., 2005, *MNRAS*, 356, 1293
 Yang X., Mo H.J., van den Bosch F.C., Pasquali A., Li C., Barden M., 2007, *ApJ*, 671, 153 (Paper I)
 Yang X., Mo H.J., van den Bosch F.C., 2008a, *ApJ*, 676, 248
 Yang X., Mo H.J., van den Bosch F.C., 2008b, preprint, arXiv:0808.0539
 Yang X., Mo H.J., van den Bosch F.C., 2008c, preprint, arXiv:0808.2526